SAKARYA UNIVERSITY
JOURNAL OF SCIENCE
e-ISSN: 2147-835X
http://www.saujs.sakarya.edu.tr

Received
02-01-2018
Accepted
10-05-2018

Doi
10.16984/saufenbilder.373735

# Role of Ag and tannin modification on photocatalytic and antibacterial properties of ZnO nanoplates

Nuray Güy*[1], Soner Çakar[2], Keziban Atacan[3]

## Abstract

In this study, photocatalytic and antibacterial activities of ZnO, Ag/ZnO, ZnO/tannin and Ag/ZnO/tannin synthesized by microwave-hydrothermal and borohydride reduction method have been investigated. The products were characterized by X-ray diffraction (XRD), field emission scanning electron microscopy (FESEM), energy dispersive spectroscopy (EDS), fourier transform infrared (FTIR) and UV–Vis diffuse reflectance/absorbance spectroscopy (DRS). Photocatalytic activities of products were explored for the degradation of malachite green (MG) dye in presence of UV light irradiation. When photocatalytic activities of them were compared, Ag/ZnO exhibited the highest photocatalytic activity. The photodegradation efficiency of 98.68% was recorded for Ag/ZnO after 30 min. The antibacterial activities of the prepared products were examined against *Escherichia coli (E. Coli)*, *Staphylococcus aureus* (*S. aureus*) and *Candida* by the well diffusion method. The results showed more excellent antibacterial activity in Ag/ZnO/tannin compared to others.

**Keywords:** Antibacterial properties, photocatalyst, Ag/ZnO, tannin

## 1. INTRODUCTION

Nowadays, industrialization is increasing rapidly in developing countries. As well as the main advantages offered by industrialization, there are some handicaps caused by it. One of these handicaps is water pollution, which is caused by industrial dyestuff, negatively affecting ecosystem and human health. As a cationic dye Malachite green (MG), is highly soluble in water and usually used in the textiles and paper industries. It is known that the use of MG damage to human and animal health, cause various types of cancer, affect respiratory and gastrointestinal systems [1,2]. Thus, appropriate method should be selected to treat wastewaters containing color pollutants such MG, before discharging to the environment [1,2]. Semiconductor photocatalysis, known as green technology, is seen as an effective method for removing toxic organic pollutants and pathogens

*Corresponding Author: nurayg@sakarya.edu.tr
[1]Sakarya University, Science & Arts Faculty, Department of Chemistry, 54187 Sakarya, Turkey
[2]Bulent Ecevit University, Science and Technology Research and Application Center (ARTMER), 67100 Zonguldak, Turkey
[3]Sakarya University, Biomedical, Magnetic and Semiconductor Materials Research Center (BIMAS-RC), 54187 Sakarya, Turkey

in wastewater [3–5]. ZnO is an attractive and promising photocatalyst, which has a wide band gap of 3.37 eV, a high exciton binding energy of 60 meV, low cost, and an eco-friendly [6,7]. Furthermore, it is a bactericide and it inhibits both Gram-positive and Gram-negative bacteria [5,7,8].

The fast recombination ratio of photoinduced charge carriers has inhibited the activiy of ZnO. So, doping of noble or transition metals, such as Ag, Au, Pt, Ni and Cu, onto ZnO can effectively enhance the photocatalytic efficiency of ZnO [5]. Among the noble metal doped ZnO photocatalysts, Ag/ZnO has drawn attention because of their abilities as effective separation of charge carriers and retardation of their recombination. The photogenerated electrons in the conduction band (CB) of ZnO can be migrated to Ag nanoparticles (NPs) because of the Schottky barrier at the Ag–ZnO interface. Thus, the Ag NPs facilitates the charge separation and enhancing the photocatalytic activity [9]. Besides, Ag NPs have unique antibacterial properties which facilitate the removal of pathogens from the water [3–5]. The modificiation of Ag NPs with ZnO is an efficient technique to generate antibacterial materials with advanced functional properties. The Gram-negative *Escherichia coli*, Gram-positive *Staphylococcus aureus* and fungi *Candida*, which usually are found as faecal contaminations in the hospital and municipal wastewaters, are the most studied microorganisms in the antibacterial applications [10,11].

Tannins, which are low cost and natural polymers, contain polyphenolic compounds of molecular weight changed between 500 and some thousands Daltons. In photocatalysis process, tannin can function as an electron trap and carrier to prolong lifetime of the electron-hole pairs. So, electron–hole recombination is effectively suppressed and the photocatalytic efficiency of the semiconductor is developed [12,13]. Antibacterial properties of tannins have been known for a long time [6,14]. The number and location of hydroxyl groups in this phenolic structure play an important role in their toxicity to microorganisms. As the number of hydroxyl groups increases, toxicity also increases. So, tannins inhibit growth of fungi, bacteria and viruses [15].

In this study, undoped ZnO, Ag/ZnO, ZnO/tannin and Ag/ZnO/tannin were synthesized by microwave-hydrothermal method. The prepared products were characterized by X-ray diffraction (XRD), field emission scanning electron microscopy (FESEM) and UV–visible diffuse reflectance spectra (UV–Vis DRS). Although Ag/ZnO nanocomposites have been extensively studied in the literature, effect of tannin modification on photocatalytic and antibacterial features of ZnO was investigated in this work. The photocatalytic performance of the products for degradation of MG under UV light irradiation and their antibacterial activities against *Escherichia coli*, *Staphylococcus aureus* and *Candida* have been systematically evaluated.

## 2. MATERIALS AND METHODS

### 2.1. Materials

Zinc chloride ($ZnCl_2$, Merck), sodium hydroxide (NaOH, Merck), silver nitrate ($AgNO_3$, Carlo Erba), sodium borohydride ($NaBH_4$, Merck), and MG (commercial grade) Mueller-Hinton agar (Merck) and ethanol (Merck) and used without further purification. Commercial tannin extract, valonia, was obtained from MİRKİM Leather and Chemical Material, Gerede/Bolu-Turkey. All compounds except MG and tannin were of reagent grade.

### 2.2. Preparation of photocatalysts

Synthesis of ZnO: The ZnO nanoplates were synthesized by microwave-assisted hydrothermal method. $ZnCl_2$ (3.66 mmol, 0.5 g) was dissolved in 10 mL of distilled water then 10 mL of NaOH (20 mmol, 0.80 g) solution was dropped and stirred for 1 h. The reaction mixture was transferred into a Teflon autoclave and treated at 160 °C for 5 min under temperature-controlled mode in a microwave oven (CEM Mars 5) operating at 700 W and then cooled at room temperature. The products were centrifuged, washed with distilled water and absolute ethanol several times and and finally, dried in an oven at 60 °C.

Synthesis of Ag/ZnO: Ag doped ZnO photocatalyts were prepared by borohydride reduction method. Required amount of the salt solution of the metal for doping was added to dispersed ZnO (1.23 mmol, 0.1 g) in 40 mL of water. The weight ratio of Ag to ZnO in this representative reaction was 5%. Then 20 mL of sodium borohydride (0.35 mmol, 0.013 g) solution as a reducing agent was dropped to the mixture and stirred for 1 h to reduce adsorbed metals ions to metallic NPs onto ZnO surface. The products were

washed distilled water and absolute ethanol several times, and then dried in an oven at 60 °C.

Synthesis of ZnO/tannin: 0.1 g tannin was dissolved into 40 mL of distilled water and $ZnCl_2$ (15.01 mmol, 2.0457 g) was added into the solution. Then, 20 mL of NaOH (80 mmol, 3.2 g) solution was dropped into the mixture and stirred for at 25 °C for 1 h. The resulting mixture was transferred into a Teflon autoclave and treated at 160 °C for 5 min under temperature-controlled mode in a microwave oven (CEM Mars 5) operating at 700 W and then cooled at room temperature. The product was washed distilled water and absolute ethanol several times, and then dried in an oven at 60 °C for 24 h.

Synthesis of Ag/ZnO/tannin: 0.1 g of ZnO/tannin was dispersed into 40 mL of distilled water. $AgNO_3$ solution was added to mixture such that the weight ratio of Ag to ZnO was 5%. Then 20 mL of sodium borohydride (0.35 mmol, 0.013 g) solution as a reducing agent was dropped to the mixture and stirred for 1 h at room temperature. The product was washed distilled water and absolute ethanol several times, and then dried in an oven at 60 °C for 24 h.

### 2.3. Characterization of photocatalysts

The prepared products were confirmed by powder X-ray diffraction (XRD, PANalytical Empyrean diffractometer with Cu Kα (λ=1.54 Å) in the 2θ angles ranging from 10 to 90. The morphologies of ZnO, Ag/ZnO, ZnO/tannin and Ag/ZnO/tannin nanocomposites were characterized by using a field emission scanning electron microscopy (FESEM, FEI QUANTA FEG 450). The surface compositions of the samples were identified by energy dispersive spectroscopy (EDS). The UV–Vis absorption spectra of the MG solution and photocatalysts were determined by using a UV-Visible spectrophotometer (UV-Vis, Shimadzu UV-2600). The diffuse reflectance spectra of the products were analyzed by using a UV-Visible spectrophotometer fitted with a diffuse reflectance attachment. The band gap energies of the nanophotocatalysts were determined by the Kubelka–Munk function, F(R) and by extrapolating the $[F(R)hv]^{1/2}$ versus photon energy (hv). Fourier Transform Infrared (FTIR) spectra of prepared photocatalysts were recorded by using a FTIR Spectrometer (Perkin Elmer FTIR Spectrum Two) in the range 400–4000 $cm^{-1}$ at room temperature.

### 2.4. Photocatalytic testing

Photocatalytic efficiencies of obtained products were examined by degradation of MG in an aqueous solution under a 100 W UV light (the strongest emission at 365 nm). For each experiment, 50 mg of photocatalyst was dispersed in 100 mL of 16 mg/L of the MG aqueous solution. Before illumination, the suspensions were stirred for 30 min in the dark to supply establishment of adsorption/desorption equilibrium of MG on surfaces of the photocatalysts in the aqueous solutions. 5 mL of the aliquots were sampled at predetermined time intervals, centrifuged and examined by recording variations in the absorption band (616 nm) in the UV–Vis spectra of MG. The percentage of degradation was determined by using the Eqs. (1) and (2) [16]:

$$\text{Degradation} = \frac{C_0\text{-}C}{C_0} \text{x} 100 \quad (1)$$

$$= \frac{A_0\text{-}A}{A_0} \text{x} 100 \quad (2)$$

where $C_0$ indicates the initial concentration after the equilibrium adsorption, C indicates the reaction concentration of MG, $A_0$ indicates the initial absorbance, and A indicates the changed absorbance of the MG at the characteristic absorption wavelength of 616 nm.

### 2.5. Antibacterial testing

The antibacterial activity of the all products were examined against Gram-negative bacteria *E. Coli*, Gram-positive bacteria *S. aureus* and fungi *Candida* by agar well diffusion method. In this study, Mueller-Hinton agar was used as a nutrient agar medium. This medium was poured into sterile Petri dishes and using sterile cottons wab, bacterial suspension was spread over the plates by spread plate method. All the products were placed on stated agar plate, followed by incubation at 37 °C for 24 h [17]. All the agar plates were visually examined for the existence of bacterial growth, and the diameter of inhibitory zones was measured in millimeter (mm).

## 3. RESULTS AND DISCUSSION

### 3.1. Characterization of photocatalysts

The phases of ZnO, Ag/ZnO, ZnO/tannin and Ag/ZnO/tannin were identified by XRD in Figure 1. As depicted in Figure 1(a), the peaks at 2θ

values of 31.7°, 34.4°, 36.2°, 47.5°, 56.6°, 62.9°, 66.4°, 68.0°, 69.1°, 72.6°, and 77.0°, indexed to (100), (002), (101), (102), (110), (103), (200), (112), (201), (004), and (202) planes of the ZnO crystal, respectively. Obviously, Ag/ZnO exhibits the usual wurtzite, just like original ZnO nanoplates, with similar peak intensities and shapes. However, the XRD patterns of Ag/ZnO illustrate diffraction peaks corresponding to the (111) and (200) facets of Ag (JCPDS cards file no.; ZnO:36-1451, Ag:04-0783), which has the face-centered cubic (fcc) structure [18]. Furthermore, similar peaks were observed in the ZnO/tannin and Ag/ZnO/tannin. But, the peak intensities only slightly decreased by modification tannin compared to the peaks of ZnO and Ag/ZnO. The average crystallite sizes of the samples were calculated by Scherrer equation ($D = 0.9\lambda/\beta \cos\theta$, where $\lambda$ is the wavelength of the radiation, $\theta$ is the diffraction angle, and $\beta$ is the corrected half width of the diffraction peak). It has been reported in the literature that ZnO powders exhibit the nature of crystals corresponding to the (100), (002) and (101) planes [19]. The average crystal sizes for samples are illustrated in Table 1. As can be seen from Table 1, Ag/ZnO has a larger crystal size than the others. Because the ionic radius of the $Ag^{+}$ (126 pm) ions substituted with the $Zn^{2+}$ ions (74 pm) in ZnO crystal, is larger than that of $Zn^{2+}$ ions. So it promotes the growth of the crystal size [18]. It is known that the crystal size influences the adsorption and the photocatalytic performance. However, our results, which are consistent with those of Zhong et al. [20] and Khataee et al. [21], showed that crystal sizes of samples caused no effect on the photocatalytic efficiency [18].

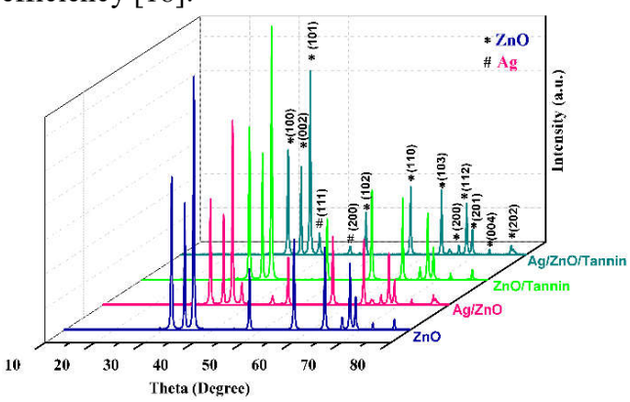


Figure 1. XRD patterns of ZnO and Ag/ZnO

Table 1. The crystal sizes of ZnO, Ag/ZnO, ZnO/tannin and Ag/ZnO/tannin

| Compound | Structure | $D_{average}$ (nm) |
|---|---|---|
| **ZnO** | Hexagonal | 29.12 |
| **Ag/ZnO** | Hexagonal | 31.23 |
| **ZnO/tannin** | Hexagonal | 25.58 |
| **Ag/ZnO/tannin** | Hexagonal | 28.02 |

Morphology analysis of the ZnO, Ag/ZnO, ZnO/tannin and Ag/ZnO/tannin were investigated by FESEM and the images are shown in Figure 2. As can be observed in Figure 2(a), ZnO shows an irregular nanoplate like structure. Figure 2(b) shows a FESEM image of the Ag/ZnO. Ag doping does not change the plate structure of ZnO. Furthermore, from Figure 2(b), we can see dispersed small Ag NPs taking place on ZnO surface. The FESEM images of ZnO/tannin and Ag/ZnO/tannin are illustrated in Figure 2(c) and Figure 2(d), respectively. As can be seen, the surfaces ZnO and Ag/ZnO nanoplates are highly coated with the tannin molecules for ZnO/tannin and Ag/ZnO/tannin [22]. Table 2 illustrates EDS analysis results for the samples to confirm element compositions of them. The results for the Ag/ZnO show Ag, Zn and O elements while it does Zn and O elements for ZnO. Furthermore, the increase in the amount of O and presence of C is evidence of tannin in the ZnO/tannin and Ag/ZnO/tannin.

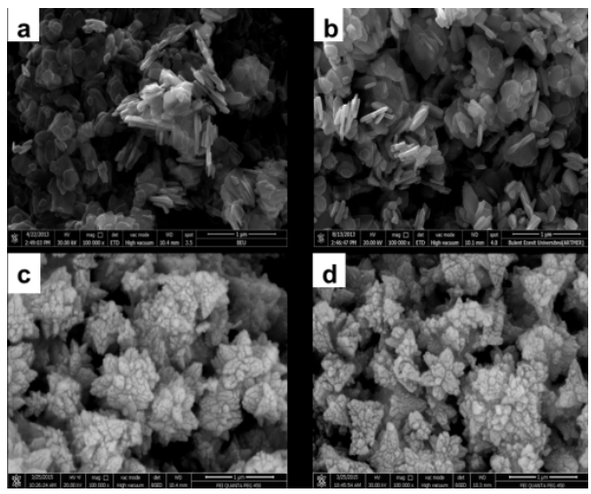


Figure 2. FESEM images of (a) ZnO, (b) Ag/ZnO, (c) ZnO/tannin and (d) Ag/ZnO/tannin

Table 2. The EDS analysis of ZnO, Ag/ZnO, ZnO/tannin and Ag/ZnO/tannin

| Elements/ (at.%) (EDS) | ZnO | Ag/ZnO | ZnO/tannin | Ag/ZnO/ tannin |
|---|---|---|---|---|
| **Zn** | 18.48 | 10.23 | 9.230 | 7.788 |
| **O** | 81.52 | 88.23 | 63.66 | 68.98 |
| **Ag** | - | 1.540 | - | 1.102 |
| **C** | - | - | 27.11 | 22.13 |
| **Total** | 100 | 100 | 100 | 100 |

The optical features of the prepared products were analyzed from the UV–Visible diffuse reflectance spectra and the results were illustrated in Figure 3. ZnO exhibits a sharp band at 377 nm, which corresponds to the ZnO nanoplates. Broad peak at 450 nm is observed in the reflectance spectra of the products representing the formation of Ag NPs. The diffuse reflectance is defined the Kulbelka-Munk function by the equation $F(R) = (1-R)^2/2R$, where R is the diffuse reflectance of the sample. This spectra supplies the calculation of the band gap of the sample with the help of the Kubelka Munk theory [23]. As can be seen in Figure 4, the band gap energies are found to be 3.23 eV for ZnO and ZnO/tannin, and 3.22 eV for Ag/ZnO, and Ag/ZnO/tannin, corresponding to UV region of the electromagnetic spectrum. According the results, the band gap energies of the nano photocatalysts change slightly with doping Ag and tannin.

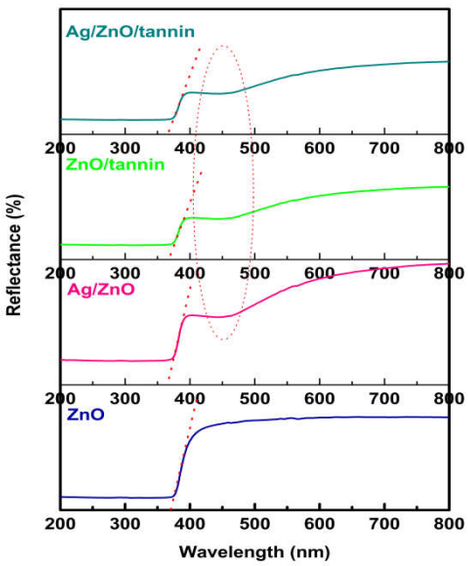


Figure 3. UV-Vis diffuse reflectance spectra of samples

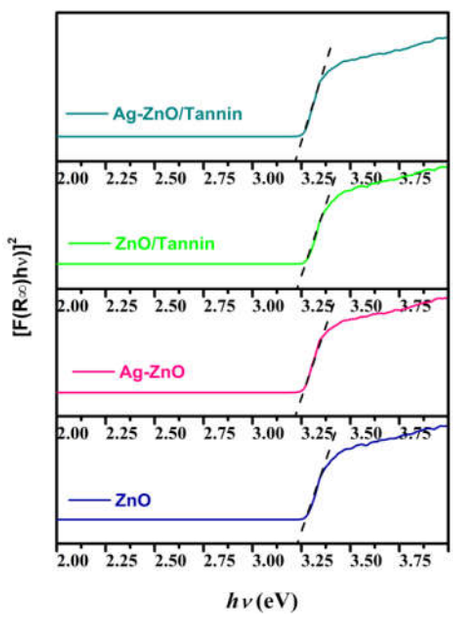


Figure 4. The plot of the transformed Kubelka–Munk function *versus* the gap energy of samples

To learn more information about the structures, FTIR spectra of ZnO, Ag/ZnO, ZnO/tannin and Ag/ZnO/tannin nanophotocatalysts were supplied and the spectra is shown in Figure 5. For the ZnO containing photocatalysts, the peak at 570 $cm^{-1}$ is assigned to the stretching vibration of the Zn–O bond. In Figure 5(c)-(d), the C=C-C stretching vibration of aromatic ring can be seen in the 1560–1400 $cm^{-1}$ region. The C-O stretching vibrations of hydrolysable tannins can be seen at 1200 $cm^{-1}$. At 800 $cm^{-1}$, C-H deformation peak has a weak intensity.

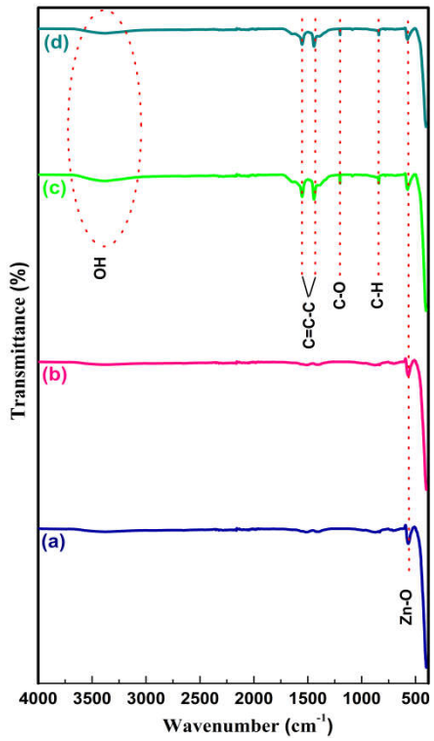


Figure 5. FTIR spectra of (a) ZnO, (b) Ag/ZnO (c) ZnO/tannin and (d) Ag/ZnO/tannin

### 3.2. Photocatalytic activity of materials

In this study, to investigate the photocatalytic efficiencies of the photocatalysts, we used MG which has the strong absorption at 616 nm. Figure 6 illustrates the time-dependent absorbance spectra of MG in the presence of ZnO, Ag/ZnO, ZnO/tannin and Ag/ZnO/tannin. As can be seen in Figure 6, MG degrades much faster in the presence of Ag/ZnO than in the presence of the other photocatalysts. Figure 7(a) exhibits the changes in the concentration of MG determined. As shown in Figure 7(a), photocatalytic activity was not observed in the absence of any catalyst under UV light. But, the degradation efficiencies for MG are about 95.8 and 98.7, 88.5, 90.7% for ZnO, Ag/ZnO, ZnO/tannin and Ag/ZnO/tannin

photocatalysts in the 30 min, respectively. Figure 7(b) illustrates the pseudo-first order kinetics of the MG photodegradation of the products. Pseudo-first order reaction kinetics is given by the following equation [19]:

$$\ln(C_t/C_0)=kt \quad (3)$$

where k is the degradation rate constant and $C_0$ and C are the concentrations of dye, initial and at the reaction time t, respectively. The pseudo-first order rate constants of the ZnO, Ag/ZnO, ZnO/tannin and Ag/ZnO/tannin are shown in Table 3. According to the results, Ag/ZnO has the highest *k* value ($91.2\text{x}10^{-6}$ $\text{min}^{-1}$) compared with others. It is claimed that the photocatalytic efficiency of the Ag/ZnO is ascribed to the presence of Ag on ZnO surface that effectively inhibits the recombination of charge carriers. Due to the SPR and synergistic effect of Ag NPs, the photoinduced electrons in the CB of ZnO flow to the surface of Ag NPs under UV light irradiation. As a result, Ag NPs serve as electron traps and retard electron-hole recombination [7,24]. However, the reason why the activities of ZnO/tannin and Ag/ZnO/tannin photocatalysts are lower than ZnO and Ag/ZnO respectively, can be explained by the tannin molecules covering the active surfaces of ZnO.

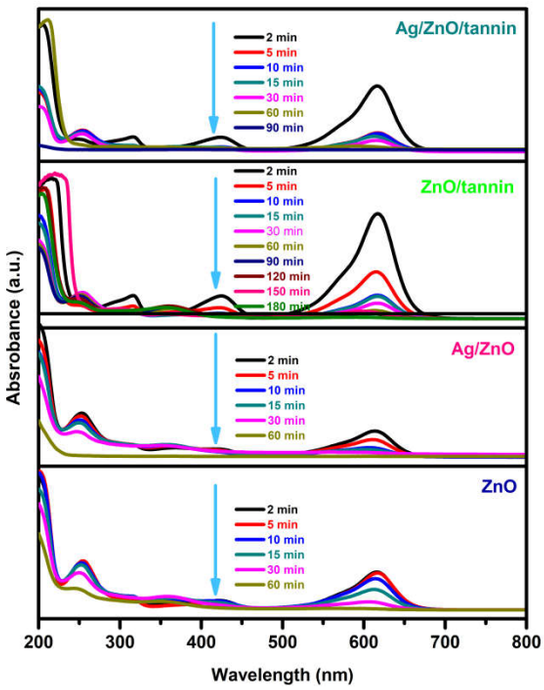


Figure 6. The absorption spectra of MG aqueous solution under UV light irradiation in the presence of samples

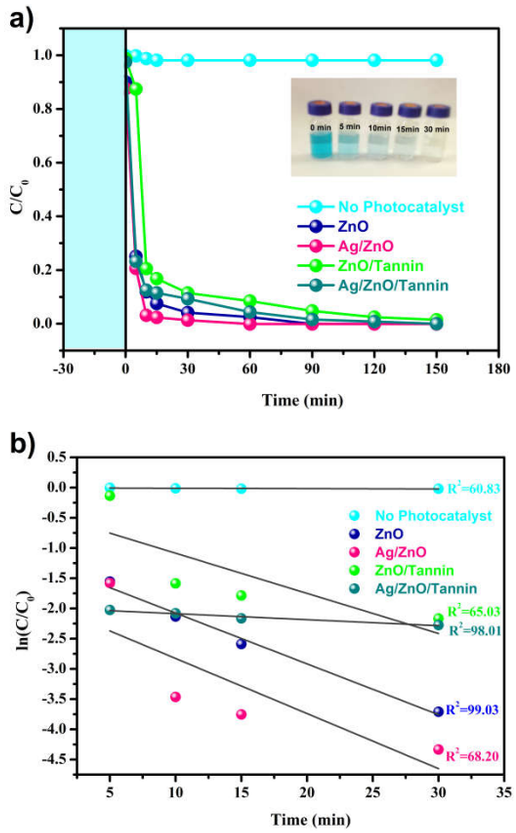


Figure 7. a) The photodegradation of MG in presence of various photocatalysts b) Pseudo-first order kinetics for MG dye

Table 3. Kinetics data of MG photodegradation in the presence of photocatalysts.

| Samples | Rate constants, *k* ($\text{min}^{-1}$) | Photodegradation ratios after 30 min irradiation (%) |
|---|---|---|
| ZnO | $84.1\text{x}10^{-6}$ | 95.85 |
| Ag/ZnO | $91.2\text{x}10^{-6}$ | 98.68 |
| ZnO/tannin | $66.3\text{x}10^{-6}$ | 88.54 |
| Ag/ZnO/tannin | $9.92\text{x}10^{-6}$ | 90.72 |

### 3.3. Photocatalytic mechanism

The Ag/ZnO exhibits an enhancement in the photocatalytic activity under UV-light irradiation compared to the other photocatalysts. Ag NPs on the ZnO surface form a schottky barrier at the Ag-ZnO interface, they trap the electrons and prevent the return to the ZnO surface, and so it extends the lifetime of the charge carriers. The possible mechanism of the Ag/ZnO for degradation of MG can be proposed as follows [9,18]:

$$ZnO + h\nu \xrightarrow{UV\ Light} ZnO(e^-_{CB} + h^+_{VB}) \quad (4)$$

$$Ag \rightarrow Ag^+ + e^- \quad (5)$$

$$e^- + O_2 \rightarrow \bullet O_2^- \quad (6)$$

$$\bullet O_2^- + H^+ \rightarrow HOO\bullet \quad (7)$$
$$2HOO\bullet \rightarrow H_2O_2 + O_2 \quad (8)$$
$$H_2O_2 + O_2 + e_{CB}^- \rightarrow O_2 + HO\bullet + OH^- \quad (9)$$
$$Ag^+ + e^- \rightarrow Ag \quad (10)$$
$$h_{VB}^+ + OH^- \rightarrow HO\bullet \quad (11)$$
$$HO\bullet + MG \rightarrow \text{Degradation products.} \quad (12)$$

Figure 8 illustrates the schematic electron-hole separation in presence Ag-ZnO system under UV light. When ZnO is illuminated by UV light, an electron ($e^-$) in the VB can be excited to the CB, leaving a hole ($h_{VB}^+$) in the VB. The photogenerated electrons migrate from ZnO to the Ag to reach fermi energy level equilibration ($E_f$) because fermi level of Ag is lower than that of ZnO [3]. Then, electrons on the Ag react with adsorbed oxygen and form more super oxide radical anion ($\bullet O_2^-$), and simultaneously, VB holes of ZnO also produce hydroxyl ($\bullet OH^-$) radical by interaction with water. Consequently, these strong radicals are used for degradation MG [3,18,24].

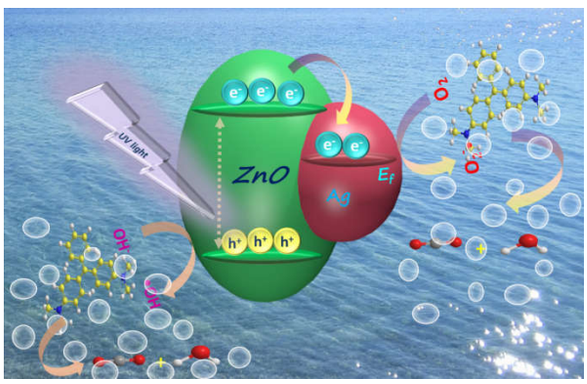


Figure 8. Schematic illustration of photocatalytic activation for MG using Ag/ZnO UV-light irradiation

### 3.4. Antibacterial activity of materials

Antimicrobial activities of the ZnO, Ag/ZnO, ZnO/tannin and Ag/ZnO/tannin were performed against *E. Coli*, *S. aureus* and *Candida*. Figure 9 illustrates the photographic images of the zone of inhibition for the products, and the diameters of the zones of inhibition are summarized in Table 3. When the diameters of the zones of inhibition (if present) for each product were compared, it was observed that Ag/ZnO/tannin nanocomposite were more effective against *E. Coli*, *S. aureus* and *Candida*. Because Ag NPs have high surface areas and unique physicochemical properties, they remarkably reduce bacterial infections [17]. Ag NPs may contact with more easily the bacterial cell membrane, causing structural changes and degradation and eventually, leading to bacterial cell death [25]. Furthermore, the diameter of the inhibition zone for Ag/ZnO is larger than that of pure ZnO. The phenolic groups which tannin molecules contain, hinder bacterial growth and protease activity via harming its cell wall and cytoplasm, so the destruction of vegetative structure of bacteria is accelerated [15,25]. As a result, Ag/ZnO/tannin has better antimicrobial activity due to the synergistic effect of combining Ag, ZnO and tannin.

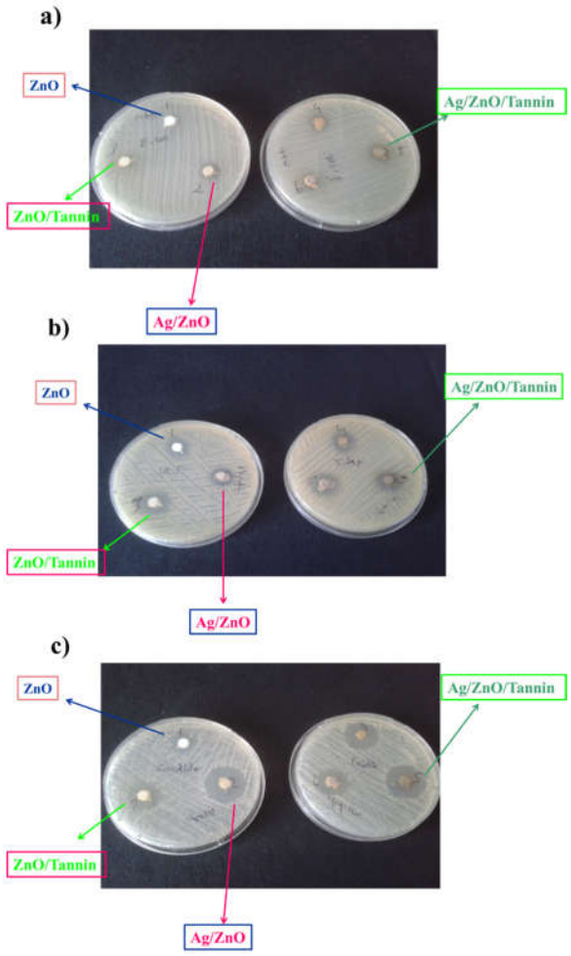


Figure 9. Inhibition zones of ZnO, Ag/ZnO, ZnO/tannin and Ag/ZnO/tannin against (a) *E. coli*, (b) *S.aureus* and (c) *Candida*.

Table 3. Antibacterial activities of ZnO, Ag/ZnO, ZnO/tannin and Ag/ZnO/tannin against pathogenic bacteria and fungal strains.

| Type of NPs | Diameter of Inhibition Zone (mm) | | |
|---|---|---|---|
| | Bacterial Strains | | Fungal Strains |
| | E.Coli | S.Aureus | Candida |
| ZnO | 0 | 9 | 12 |
| Ag/ZnO | 12 | 14 | 20 |
| ZnO/tannin | 10 | 11 | 18 |
| Ag/ZnO/tannin | 12 | 15 | 24 |

## 5. CONCLUSIONS

In summary, ZnO, Ag/ZnO, ZnO/tannin and Ag/ZnO/tannin were synthesized by microwave-hydrothermal method. These nanocomposites have potential applications in both photodegradation of MG and inhibition of bacteria and fungi. Ag/ZnO exhibits better photocatalytic efficiency for MG than other photocatalysts due to hindering electron hole pair recombination by Ag NPs and enhancing of the performance of Ag/ZnO by surface plasmon resonance of them. In the antibacterial tests, due to the strong interaction between metallic Ag, tannin and ZnO, Ag/ZnO/tannin exhibited enhanced and synergistic antibacterial activities for *E. coli*, *S. aureus* and *Candida*.

## ACKNOWLEDGMENTS

We would like to thank Prof. Dr. Oğuz Karabay for his helping antibacteriel studies in Faculty of Medicine at Sakarya University.

## REFERENCES

[1] M. Rahmani, M. Kaykhaii, M. Sasani, "Application of Taguchi L16 design method for comparative study of ability of 3A zeolite in removal of Rhodamine B and Malachite green from environmental water samples", *Spectrochim. Acta Part A Mol. Biomol. Spectrosc.,* vol. 188, pp. 164–169, 2018.

[2] X. Zhang, M. Wang, L. Lin, G. Xiao, Z. Tang, X. Zhu, "Synthesis of novel laccase-biotitania biocatalysts for malachite green decolorization", J. *Biosci. Bioeng.* In Press, 2018.

[3] N.L. Gavade, A.N. Kadam, Y.B. Gaikwad, M.J. Dhanavade, K.M. Garadkar, "Decoration of biogenic AgNPs on template free ZnO nanorods for sunlight driven photocatalytic detoxification of dyes and inhibition of bacteria," *J. Mater. Sci. Mater. Electron,* vol. 27, pp. 11080–11091, 2016.

[4] B. Pant, M. Park, H.Y. Kim, S.J. Park, "Ag-ZnO photocatalyst anchored on carbon nanofibers: Synthesis, characterization, and photocatalytic activities," *Synth. Met*., vol. 220, pp. 533–537, 2016.

[5] Z. Li, F. Zhang, A. Meng, C. Xie, J. Xing, "ZnO/Ag micro/nanospheres with enhanced photocatalytic and antibacterial properties synthesized by a novel continuous synthesis method," *RSC Adv*., vol. 5, pp. 612–620, 2015.

[6] R.T. Al-ani, N. Mohammed, V.M. Atheer, M.P. D, "Antibacterial Activity of Tannins Extracted from Some Medicinal Plants in vitro," *Department of Biochemistry, Medicine College, Al-Anbar University, Ramadi, IRAQ*, vol. 6, no. 1, pp. 8876-8882, 2008.

[7] C. Karunakaran, V. Rajeswari, P. Gomathisankar, "Enhanced photocatalytic and antibacterial activities of solgel synthesized ZnO and Ag-ZnO," *Mater. Sci. Semicond. Process*., vol. 14, pp. 133–138, 2011.

[8] G. Nagaraju, Udayabhanu, Shivaraj, S.A. Prashanth, M. Shastri, K. V. Yathish, C. Anupama, D. Rangappa, "Electrochemical heavy metal detection, photocatalytic, photoluminescence, biodiesel production and antibacterial activities of Ag–ZnO nanomaterial," *Mater. Res. Bull*., vol. 94, pp. 54–63, 2017.

[9] W. Lu, G. Liu, S. Gao, S. Xing, J. Wang, "Tyrosine-assisted preparation of Ag/ZnO nanocomposites with enhanced photocatalytic performance and synergistic antibacterial activities," *Nanotechnology*, vol. 19, pp. 445711- 445721, 2008.

[10] C. Piccirillo, R.A. Pinto, D.M. Tobaldi, R.C. Pullar, J.A. Labrincha, M.M.E. Pintado, P.M.L. Castro, "Light induced antibacterial activity and photocatalytic properties of $Ag/Ag_3PO_4$ -based material of marine origin", *Journal Photochem. Photobiol. A Chem*., vol. 296, pp. 40–47, 2015.

[11] R. Van Grieken, J. Marugán, C. Pablos, L. Furones, A. López, "Comparison between the photocatalytic inactivation of Gram-positive E . faecalis and Gram-negative E . coli faecal contamination indicator microorganisms", *Applied Catal. B, Environ*., vol. 100, pp. 212–220, 2010

[12] X. Huang, Y. Wang, X. Liao, B. Shi, Adsorptive recovery of $Au^{3+}$ from aqueous solutions using bayberry tannin-immobilized mesoporous silica", *J. Hazard. Mater.,* vol. 183, pp. 793–798, 2010.

[13] S. Ayhan, M. Özacar, "Competitive biosorption of $Pb^{2+}$, $Cu^{2+}$ and $Zn^{2+}$ ions from aqueous solutions onto valonia tannin

resin," *Journal of Hazardous Materials*, vol. 166, pp. 1488–1494, 2009.

[14] K. Tomiyama, Y. Mukai, M. Saito, K. Watanabe, H. Kumada, T. Nihei, N. Hamada, T. Teranaka, "Antibacterial Action of a Condensed Tannin Extracted from Astringent Persimmon as a Component of Food Addictive Pancil PS-M on Oral Polymicrobial Biofilms," *Biomed Res. Int.,* vol. 2016, pp. 1-7, (2016).

[15] S.M. Çolak, B.M. Yapici, A.N. Yapici, "Determination of antimicrobial activity of tannic acid in pickling process," *Rom. Biotechnol. Lett.,* vol. 15, pp. 5325–5330, 2010.

[16] Y. Chang, J. Xu, Y. Zhang, S. Ma, L. Xin, L. Zhu, C. Xu, "Optical Properties and Photocatalytic Performances of Pd Modified ZnO Samples," *J. Phys. Chem. C*, vol. 113, pp. 18761–18767, 2009.

[17] K. Atacan, M. Özacar, "Investigation of antibacterial properties of novel papain immobilized on tannic acid modified Ag/$CuFe_2O_4$ magnetic nanoparticles," *Int. J. Biol. Macromol*., vol. 109, pp. 720–731, 2018.

[18] N. Güy, M. Özacar, "The influence of noble metals on photocatalytic activity of ZnO for Congo red degradation," *Int. J. Hydrogen Energy,* vol. 41, pp. 20100–20112, 2016.

[19] Şenay Şen Türkyılmaz, N. Güy, M. Özacar, "Photocatalytic efficiencies of Ni, Mn, Fe and Ag doped ZnO nanostructures synthesized by hydrothermal method: The synergistic/antagonistic effect between ZnO and metals," *J. Photochem. Photobiol. A Chem.*, vol. 341, pp. 39–50, 2017.

[20] J.B. Zhong, J.Z. Li, X.Y. He, J. Zeng, Y. Lu, W. Hu, K. Lin, "Improved photocatalytic performance of Pd-doped ZnO", *Curr. Appl. Phys.*, vol. 12, pp. 998–1001, 2012.

[21] A. Khataee, R. Darvishi, C. Soltani, Y. Hanifehpour, M. Safarpour, H.G. Ranjbar, S.W. Joo, "Synthesis and Characterization of Dysprosium-Doped ZnO Nanoparticles for Photocatalysis of a Textile Dye under Visible Light Irradiation", *Ind. Eng. Chem. Res.,* vol. 53, pp. 1924−1932, 2014.

[22] S. Wu, P. Wang, Y. Cai, D. Liang, Y. Ye, Z. Tian, J. Liu, C. Liang, "Reduced graphene oxide anchored magnetic $ZnFe_2O_4$ nanoparticles with enhanced visible-light photocatalytic activity," *RSC Adv.*, vol. 5, pp. 9069–9074, 2015.

[23] Z. Yang, Y. Wan, G. Xiong, D. Li, Q. Li, "Facile synthesis of $ZnFe_2O_4$/reduced graphene oxide nanohybrids for enhanced microwave absorption properties," *Mater. Res. Bull.*, vol. 61, pp. 292–297, 2015.

[24] V. Vaiano, M. Matarangolo, J.J. Murcia, H. Rojas, J.A. Navío, M.C. Hidalgo, "Enhanced photocatalytic removal of phenol from aqueous solutions using ZnO modified with Ag," *Appl. Catal. B Environ*. vol. 225, pp. 197–206, 2018.

[25] S.P. Adhikari, H.R. Pant, J.H. Kim, H.J. Kim, C.H. Park, C.S. Kim, "One pot synthesis and characterization of Ag-ZnO/g-$C_3N_4$ photocatalyst with improved photoactivity and antibacterial properties," *Colloids Surfaces A Physicochem. Eng. Asp*., vol. 482, pp. 477–484, 2015.